Wide angle crystal spectrometer for angularly and spectrally resolved x-ray scattering experiments

AIP | Review of Scientific Instruments

Wide angle crystal spectrometer for angularly and spectrally resolved x-ray scattering experiments

E. García Saiz, F. Y. Khattak, G. Gregori, S. Bandyopadhyay, R. J. Clarke et al.

Citation: Rev. Sci. Instrum. **78**, 095101 (2007); doi: 10.1063/1.2783773
View online: http://dx.doi.org/10.1063/1.2783773
View Table of Contents: http://rsi.aip.org/resource/1/RSINAK/v78/i9
Published by the American Institute of Physics.

Wide angle crystal spectrometer for angularly and spectrally resolved x-ray scattering experiments

E. García Saiz[a] and F. Y. Khattak
School of Mathematics and Physics, Queen's University of Belfast, Belfast BT7 1NN, United Kingdom

G. Gregori
Central Laser Facility, Rutherford Appleton Laboratory, Chilton, Didcot OX11 0QX, United Kingdom and Clarendon Laboratory, University of Oxford, Oxford OX1 3PU, United Kingdom

S. Bandyopadhyay, R. J. Clarke, and B. Fell
Central Laser Facility, Rutherford Appleton Laboratory, Chilton, Didcot OX11 0QX, United Kingdom

R. R. Freeman
Department of Physics, The Ohio State University, Columbus, Ohio 43210, USA

J. Jeffries
Central Laser Facility, Rutherford Appleton Laboratory, Chilton, Didcot OX11 0QX, United Kingdom

D. Jung
Central Laser Facility, Rutherford Appleton Laboratory, Chilton, Didcot OX11 0QX, United Kingdom and Institut für Kernphysik, Technische Universität Darmstadt, Schloßgartenstr. 9, 64289 Darmstadt, Germany

M. M. Notley
Central Laser Facility, Rutherford Appleton Laboratory, Chilton, Didcot OX11 0QX, United Kingdom

R. L. Weber and L. van Woerkom
Department of Physics, The Ohio State University, Columbus, Ohio 43210, USA

D. Riley
School of Mathematics and Physics, Queen's University of Belfast, Belfast BT7 1NN, United Kingdom

(Received 25 June 2007; accepted 21 August 2007; published online 13 September 2007)

A novel wide angle spectrometer has been implemented with a highly oriented pyrolytic graphite crystal coupled to an image plate. This spectrometer has allowed us to look at the energy resolved spectrum of scattered x rays from a dense plasma over a wide range of angles (~30°) in a single shot. Using this spectrometer we were able to observe the temporal evolution of the angular scatter cross section from a laser shocked foil. A spectrometer of this type may also be useful in investigations of x-ray line transfer from laser-plasmas experiments. © *2007 American Institute of Physics.* [DOI: 10.1063/1.2783773]

I. INTRODUCTION

Diagnostics of hot and dense matter are important for the experimental characterization of plasmas found in inertial confinement fusion experiments[1] and laboratory astrophysics.[2] In recent years, x-ray scattering[3–6] has been proposed as a powerful method to investigate the equation of state of such systems in order to extract both microscopic (i.e., temperatures and densities) as well as structural properties. While spectrally resolved scattering[3,4] can be implemented for accurate measurements of the electron density and temperature, angularly resolved scatter[5,6] allows the detection of the long range order as in x-ray diffraction experiments. In our previous work with angularly resolved x-ray scatter from plasmas, we have used the direct detection of scattered photons with a charge coupled device (CCD) chip.[5,6] This was achievable because the CCD is sensitive enough to detect a single x-ray photon with better than 200 eV energy resolution[7,8] and a histogram of the signal in the individual pixels can be utilized as a spectrum, allowing separation of the quasimonochromatic scatter signal from the continuum x-ray background from the sample plasma. By placing the chip close to the experiment and making histograms of subareas of the chip, an angular variation in scatter was investigated. Such experiments may play a useful role in investigating the properties of warm and hot dense matter.[9] However, this method depends on filtering the signal into the CCD to the point that the chances of an individual pixel receiving more than one x-ray photon are small. This places restrictions on the experiments, particularly on the plasma conditions of the sample plasma and creates a need to eliminate all possible sources of stray photons, whatever their physical location within the target chamber. While this technique has proven successful, due to limited size of CCD chips, measurements over a large range of scattering angles requires multiple shots with the detector being moved after

[a]Electronic mail: egarciasaiz01@qub.ac.uk

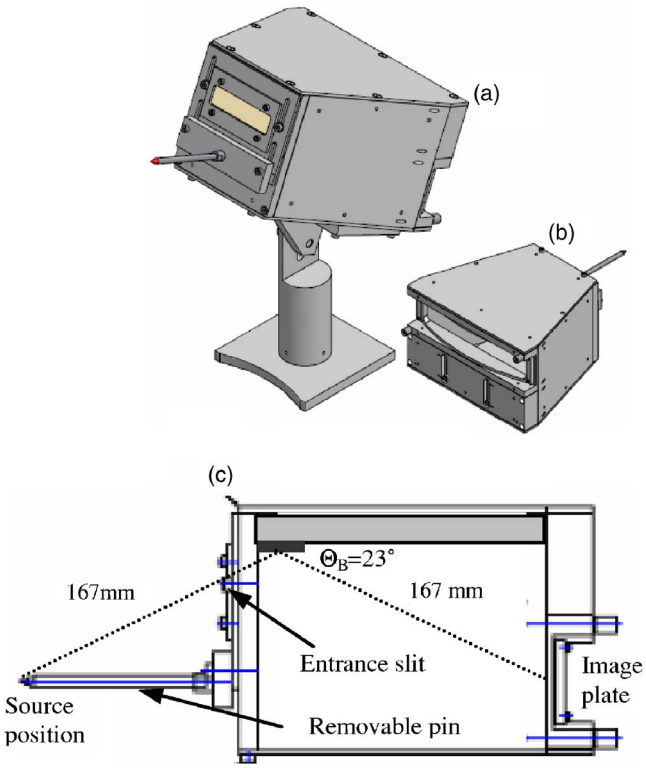

FIG. 1. (a) Front view of spectrometer on articulated mount. (b) Rear view showing the detail for the mounting for the ionization potential. (c) Cut-away section of the spectrometer showing the path of the x rays, distances, and removable pin used for alignment purposes.

each shot. In addition the spectral resolution achieved in a single photon counting detector is not sufficient to distinguish between elastically and inelastically scattered x rays.

II. INSTRUMENT DESCRIPTION

In this work, we have deployed an alternative instrument that allows simultaneous detection of scattered x rays over a wide range of angles with good spectral resolution, thus avoiding the problem of changing the position of the CCD after each shot. This also has the advantage over direct CCD detection that there is spectral dispersion that helps to separate the quasimonochromatic scatter signal from the continuum background. This improvement in the signal-to-noise ratio will allow the extension of the techniques to more extreme plasma conditions, as well as use of higher driving laser intensities to create the sample. Figure 1 shows a diagram of our wide-angle spectrometer. The instrument consists of a highly oriented pyrolytic graphite (HOPG) crystal[10,11] with a width of 100 mm in the sagittal (nonspectral) direction and mosaic spread of nominally $3.5° \pm 1.5°$ (*ZYH* grade). The crystal is placed symmetrically between the source and an image plate,[12,13] which is a required condition in order to achieve mosaic focusing. In experiments conducted at the Vulcan laser facility at the Rutherford Appleton Laboratory (UK), we were able to show that with this instrument we can collect simultaneously the angular variation in scatter, as well as spectral information, to distinguish between elastic scatter from the inelastic components that relate to bound-free Compton scatter features and free electron scatter features.[14]

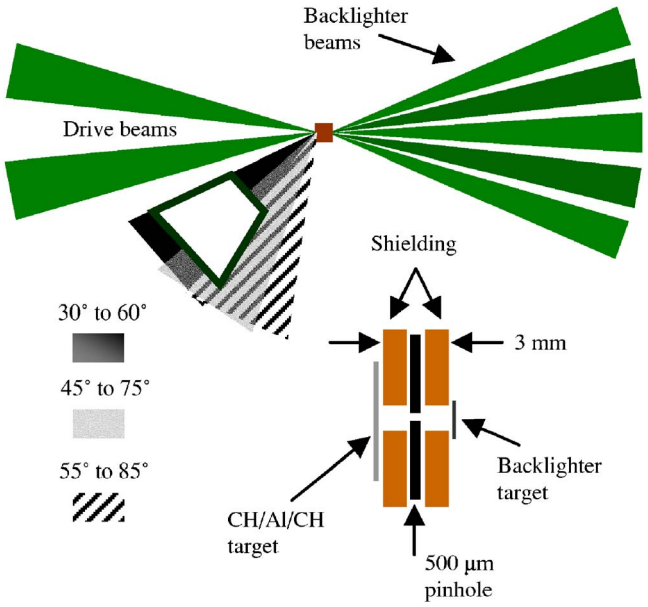

FIG. 2. Schematic diagram for the experimental arrangement, showing beam distribution, target position and spectrometer positions (up). Schematic diagram of the target (down).

As can be seen in Fig. 1, the HOPG crystal is enclosed in an Al box of dimensions 156 mm × 240 mm × 191 mm covered with a layer of lead ~1 mm thick to shield high energy x ray and gamma rays generated in the laser-plasma interaction. This sits on an articulated pedestal to allow positioning *in situ*. The aperture at the front is provided with a holder allowing the fixing of appropriate filtering. There is also a fitting for a pointer to allow accurate placement of the spectrometer relative to the source, as seen in the cut-away diagram. A holder in the back of the spectrometer allows the attachment of the detector. The original design was intended for use with an image plate as a detector, placed on a holder attached to the back of the spectrometer to have an exposed area of dimensions 42 mm × 195 mm. The image plate used in this work was Fuji BAS-TR.[15] An adaptor for a CCD camera was built, though reducing the angle detection due to the camera chip size—this was not deployed in the current experiment. A mobile Al block inside the box allowed positioning of the crystal to match the required Bragg angle; in this case 23° (for Ti He-α radiation). The distance from source to crystal was set at ~167 mm. Due to the large dimension of the crystal along the sagittal axis (100 mm), this allowed the collection of all the x rays incoming to the spectrometer within a fan of angles covering ~30°. The image plate was placed the same distance from the crystal so as to take advantage of the mosaic focusing in the spectral direction of HOPG.[10] The articulated mount, as seen in Fig. 1, allowed deployment to capture x rays scattered in the horizontal plane of the experiment.

III. APPLICATION

Figure 2 shows schematically how the spectrometer was

used in a scatter experiment and the arrangement of the beams as viewed from above. The six main cluster beams from the Vulcan laser were used to drive a backlighter foil of 6 μm Ti in order to generate an intense burst of x rays. In our experiment the laser beams were frequency doubled to 0.527 μm, with a ~1 ns long flat topped pulse delivering ~100 J per beam with intensity $I=2\times10^{15}$ W cm^{-2}. Two additional beams, again at 0.527 μm with ~1.2 ns pulse duration (with intensity $I=7\times10^{12}$ W cm^{-2} on target), were used to generate the plasma state of interest by driving a shock into the sample foil, a CH/Al/CH sandwich of 5/8/5 μm thicknesses. Analysis of the data collected will be published in a later article. By interaction with the laser beam, the titanium foils produce a hot plasma which emits at the Ti He-α line group. This creates a quasimonochromatic source, which is collimated by placing a pinhole in between the Ti source and the sample foil (as shown schematically in Fig. 2). The distance between the pinhole and the Ti plasma is set such as the spray of x-ray photons impinging the sample cover ~9.5° of total divergence. This is determines the minimum angular resolution achievable in our scattering experiment.

IV. INSTRUMENT CALIBRATION

For the proper analysis of the measured data, accurate calibration of the detector is required. The response of the spectrometer as a function of angular position along the image plate is not necessarily uniform. This is partly because the crystal is flat and not shaped to form an arc, so that x rays impinge at different angles to the plane of the surface. It is also because the nature of HOPG is that there are sometimes nonuniformities in internal structure.[10,11] We have tested the response with calibration shots at the wavelength used in the experiment (2.61 Å).

In order to correctly interpret the mosaic response of the crystal we have carried out a full line tracing calculation of the spatial (sagittal) and spectral distribution of the Bragg diffracted x rays at the detector plane. The simulation has been performed using the integrated package XOP/SHADOW,[16] assuming a point source emitting two narrow lines of equal intensity at the position of the ^1P resonance line and the ^3P "intercombination" line. The result is plotted in Fig. 3(a), which clearly shows the blue wing of the spectrum in the image plane due to depth broadening effects.[17] We also notice that due to this asymmetrical broadening, emission lines of equal intensity appear to have different strength for proper line ratio measurement this effect has to be accounted for.

Figure 3(b) shows a calibration shot taken with a ~1 ns long beam focused onto a Ti foil at the sample position. The crystal was set with a Bragg angle of 23° to detect to He-α line group ($1s-2p$ ^1P line and associated satellites) at about 2.61 Å (4.75 keV). We can see from the full width at half maximum (FWHM) of the resonance line that spectral resolution of $E/\Delta E\sim190$ was achieved, allowing the ^1P resonance line and the ^3P intercombination lines, which are separated by ~12 mÅ, to be resolved. This is in good agreement with the XOP/SHADOW simulation. The line-outs of the integrated He-α along the angular direction show a broad peak

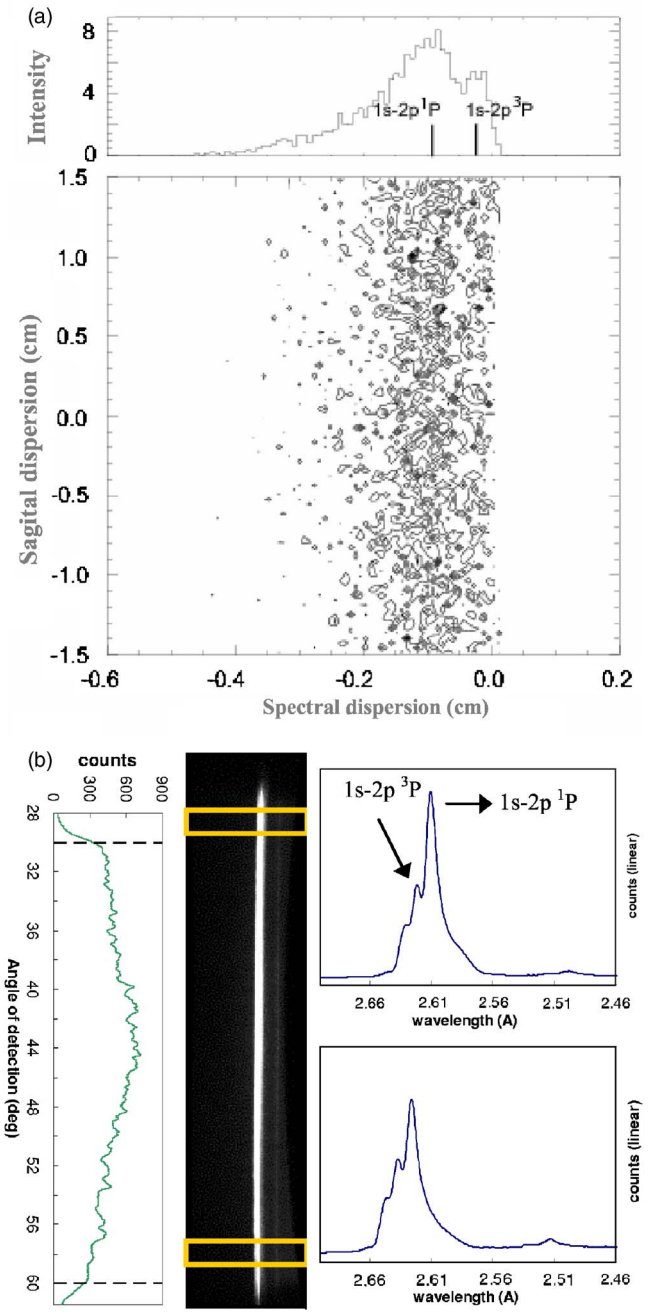

FIG. 3. (a) Line tracing calculation of the diffracted x-ray using the XOP/SHADOW package. Effect of the mosaic nature of the crystal is fully accounted in the simulation. The plot corresponds to the central region of the image plane: a sagittal coverage of 3 cm is equivalent to ~5.1° in the angular coverage. The simulation assumes a point source emitting two lines of equal intensity at the position of the He-α resonance and intercombination lines. (b) Calibration shot image with a vertical profile taken along the angular direction with dotted lines excluding edge detection due to geometrical configuration (left) and two horizontal profiles (right) along the spectral direction taken from the drawn boxes.

in the center when integrated across the spectrum. Positioning the spectrometer to sample emission at different angles relative to the plane of the laser-plasma target gave similar results, indicating absence of opacity effects in the calibration signal. In order to verify that indeed opacity effects are playing no role, we have taken line-outs using just the peak intensity of the intercombination line and found very similar behavior. In Fig. 4, we show the ratio of the resonance to

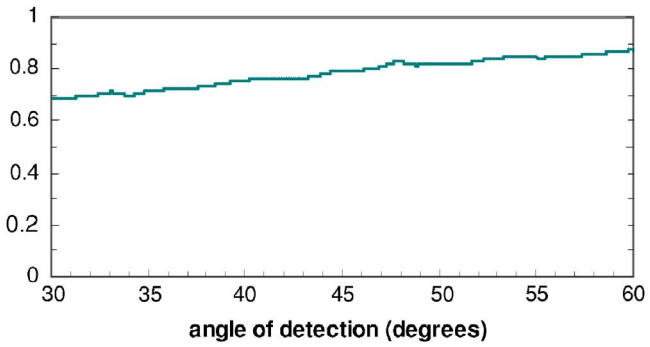

FIG. 4. Ratio of the intercombination and the resonance lines along the angular range of the detector.

intercombination line, corrected for instrument effects [as shown in Fig. 3(a)] along the angular direction of the spectrometer. We can see that there is a small variation that indicates some opacity effects, but only weakly. It is perhaps unsurprising that there is little variation with angle since the expected expansion of the plasma (>100 μm), in this case, is similar to the focal spot size and so the expansion is not planar but more spherical in nature.

In addition to the mosaic focusing in the spectral direction that allows quite good resolution, as seen before, there is expected to be a mosaic defocusing effect in the plane perpendicular to the diffraction plane (the sagittal plane), which leads to a spread in the angular direction of the spectrometer. This should be given by $\sim 2\tau \sin \theta_B$ where τ is the mosaic spread and θ_B is the Bragg angle.[11] In our case we expect a FWHM spread of ~2.6° which is significantly less than the angular resolution limit determined by the experimental geometry (i.e., the pinhole position between Ti plasma and sample foil) as discussed before. We have investigated the angular spread with a series of tests carried out with a 15 mJ, 15 ps laser by integrating several thousand tight focus shots ($\sim 5 \times 10^{13}$ W cm^{-2} at 532 nm) on a moving Ti foil. Figure 5 shows the projected intensity onto the image plate after a 1 mm wide slit was attached to the entrance of the spectrometer. By comparing the width of the image to the expected

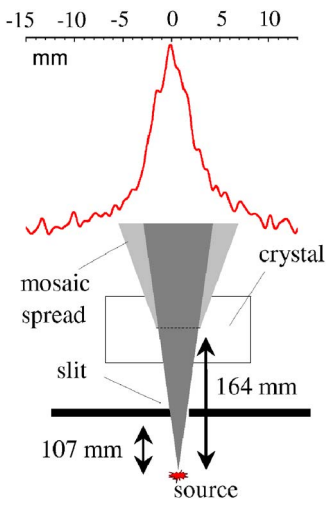

FIG. 5. Projected image of a 1 mm slit placed between the source and crystal with upper scale showing the size in millimeters.

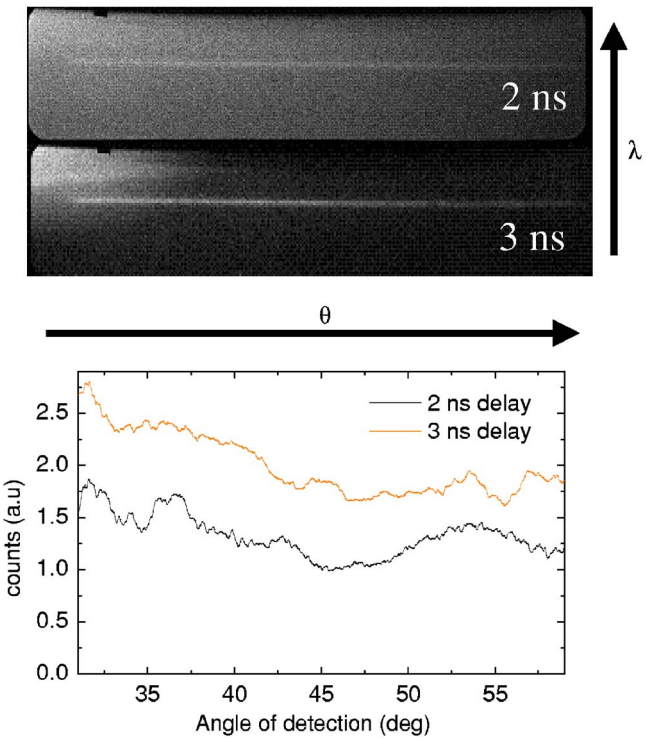

FIG. 6. Raw scatter data from the experiment at 2 and 3 ns delay. The angular range of detection was from 30 to 60 deg from the backlighter beams direction in the horizontal plane (upper image). Processed data showing the evolution of the scattered signal along the angular range (lower image).

projection in the absence of mosaic spread we estimate the mosaic spread as $\tau = 2.7 \pm 0.3°$, which is within the expected nominal value of the mosaic spread as supplied by the manufacturer. Measurements with a sharp edge instead of the slit mentioned earlier were also made achieving similar results.

In Fig. 6 we have plotted the measured data for a scattering experiment as outlined in Fig. 2. The probe x rays are generated from the bright source of the He-α photons with $\sim 3 \times 10^{12}$ photons/J.[18,19] The number of scattered photons in this experiment is estimated at $\sim 10^9$ photons/sr. With an integrated reflectivity of $\sim 2 \times 10^{-3}$ rad of the HOPG crystal we expect to gather $\sim 3 \times 10^5$ photons in a resolution element subtending 9.5° on the image plate. This translates into an expected peak flux of ~30 photons/50 μm^2 for the resonance line. This is easily enough to create a detectable signal[12,15] and the linearity has been checked for this regime. The detective quantum efficiency for this type of image plate has not been measured at 4.75 keV but it has been measured to be 3–10% at low fluence for ~1.5 and 5.9 keV photons.[12,15]

In Fig. 6 we have plotted the scatter line-outs, at different time delays between the backlighter beam on the Ti foil and the beams on the CH/Al/CH foil, ranging from 1 to 3 ns after the shock drive pulse. The response of the instrument as determined from the calibration spectrum has been deconvolved from the line-outs. We can see that there is a significant change in the scatter cross section with beam delay as the plasma moves from higher to lower density; illustrating one important application of the spectrometer. A complete history of the experiment, with data obtained at different

times and angular positions, along with modeling of the plasma conditions and comparison with expected scatter profiles will follow in a later article.

V. CONCLUSION

In summary, we have demonstrated an instrument that is capable of delivering, simultaneously, spectral and angular resolution in scattered x rays from dense plasma. Even with the use of a subkilojoule laser to generate the scatter source, we have achieved a high level of counts on the image plates, typically, 400 with the scatter shots. This indicates that with a shorter backlighter pulse and the consequent drop in photon numbers, we should still be able to take scatter profiles, with better temporal resolution. A more compact design for placement closer to the target is planned and should also help to enhance the sensitivity. The data in Fig. 4, comparing signal from the resonance and intercombination lines, indicate that another possible use is in the evaluation of opacity effects in laser-plasmas experiments, though for improvement of the accuracy it would be more adequate to have a calibration of the instrument response in a more controlled situation. This was already attempted with a Fe^{55} (5.9 keV) radioactive source, but its signal was not strong enough.

This work was supported in part by EPSRC-GB Grant No. EP/C001869/1 and by the Science and Technology Facilities Council of the United Kingdom. The authors thank the Vulcan operation, engineering, and target fabrication groups for their support during the experiment.

[1] J. D. Lindl, *Inertial Confinement Fusion* (Springer, New York, 1998).
[2] B. A. Remington, R. P. Drake, and D. D. Ryutov, Rev. Mod. Phys. **78**, 755 (2006).
[3] S. H. Glenzer, G. Gregori, R. W. Lee, F. J. Rogers, S. W. Pollaine, and O. L. Landen, Phys. Rev. Lett. **90**, 175002 (2003).
[4] S. H. Glenzer, O. L. Landen, P. Neumayer, R. W. Lee, K. Kidman, S. W. Pollaine, R. J. Wallace, G. Gregori, A. Holl, T. Bornath, R. Thiele, S. Schwarz, W. D. Kraeft, and R. Redmer, Phys. Rev. Lett. **98**, 065002 (2007).
[5] N. C. Woolsey, D. Riley, and E. Nardi, Rev. Sci. Instrum. **69**, 418 (1998).
[6] D. Riley, N. C. Woolsey, D. McSherry, and E. Nardi, J. Quant. Spectrosc. Radiat. Transf. **65**, 463 (2000).
[7] K. Hashimotodani, T. Toneri, S. Kitamoto, H. Tsunemi, K. Hayashida, E. Miyata, M. Ohtani, R. Asakura, K. Katayama, T. Kohmura, J. Hiraga, H. Katayama, M. Shoho, K. Kinugasa, T. Imayoshi, Y. Sumi, and Y. Ohono, Rev. Sci. Instrum. **69**, 3746 (1998).
[8] K. J. McCarthy, A. Owens, and A. Keay, Nucl. Instrum. Methods Phys. Res. A **384**, 403 (1997).
[9] R. Davidson, *Frontiers in High Energy Density Physics: The X-Games of Contemporary Science* (The National Academies Press, Washington, 2003).
[10] A. K. Freund, A. Munkholm, and S. Brennan, Proc. SPIE **2856**, 68 (1996).
[11] M. Sánchez del Río, M. Gambaccini, G. Pareschi, A. Taibi, A. Tuffanelli, and A. Freund, Proc. SPIE **3448**, 246 (1998).
[12] S. G. Gales and C. D. Bentley, Rev. Sci. Instrum. **75**, 4001 (2004).
[13] Y. Amemiya, J. Synchrotron Radiat. **2**, 13 (1995).
[14] G. Gregori, S. H. Glenzer, W. Rozmus, R. W. Lee, and O. L. Landen, Phys. Rev. E **67**, 026412 (2003).
[15] I. J. Paterson, R. J. Clarke, G. Gregori, and N. C. Woolsey (unpublished).
[16] M. Sanchez del Río and R. J. Dejus, Proc. SPIE **3152**, 148 (1997).
[17] A. Pak *et al.*, Rev. Sci. Instrum. **75**, 3747 (2004).
[18] D. W. Phillion and C. J. Hailey, Phys. Rev. A **34**, 4886 (1986).
[19] D. Riley, N. C. Woolsey, D. McSherry, F. Y. Khattak, and I. Weaver, Plasma Sources Sci. Technol. **11**, 484 (2002).